Supporting Information

Fabrication of a Core-shell-type Photocatalyst via Photodeposition of Group IV and V Transition Metal Oxyhydroxides: An Effective Surface Modification Method for Overall Water Splitting

Tsuyoshi Takata[†*], Chengsi Pan[†], Mamiko Nakabayashi[‡,¶], Naoya Shibata[‡] and Kazunari Domen[†,§,¶*]

[†] Global Research Center for Environment and Energy based on Nanomaterials Science (GREEN), National Institute for Materials Science (NIMS), 1-1 Namiki, Tsukuba-city, Ibaraki 305-0044, Japan

[‡] Institute of Engineering Innovation, School of Engineering, The University of Tokyo, 2-11-16, Yayoi, Bunkyo-ku, 113-8656, Japan

[§] Department of Chemical System Engineering, School of Engineering, The University of Tokyo, 7-3-1 Hongo, Bunkyo-ku 113-8656, Japan

[¶] Japan Technological Research Association of Artificial Photosynthetic Chemical Process (ARPChem), 5-1-5 Kashiwanoha, Kashiwa-city, Ciba 227-8589, Japan

*corresponding authors,
e-mail: TAKATA.Tsuyoshi@nims.go.jp, domen@chemsys.t.u-tokyo.ac.jp

SI1 $SrTiO_3$:Sc

In the present study, $SrTiO_3$ replaced with 5 at%-Sc^{3+} at Ti^{4+}-site was employed as a model photocatalyst for overall water splitting. We previously demonstrated that defect engineering by doping of $SrTiO_3$ photocatalyst with low valence cations was effective for remarkably enhancing phototocatalytic activity.* In that study, we reported the results of Na^+/Sr^{2+}- and Ga^{3+}/Ti^{4+}-substitutions as examples of enhanced photocatalysis. After the report, we found that Sc^{3+}/Ti^{4+}-substitution was more effective at enhancing water-splitting activity than the reported two cases. We selected a Sc^{3+}/Ti^{4+}-substituted sample in the present study because of its high activity and good reproducibility. Since the $SrTiO_3$:Sc photocatalyst has been unpublished, its UV-Vis DRS and photocatalytic activity are shown in Fig. S1 as a basic information, in comparison with the $SrTiO_3$:Na sample.

*Reference No 27 in the manuscript

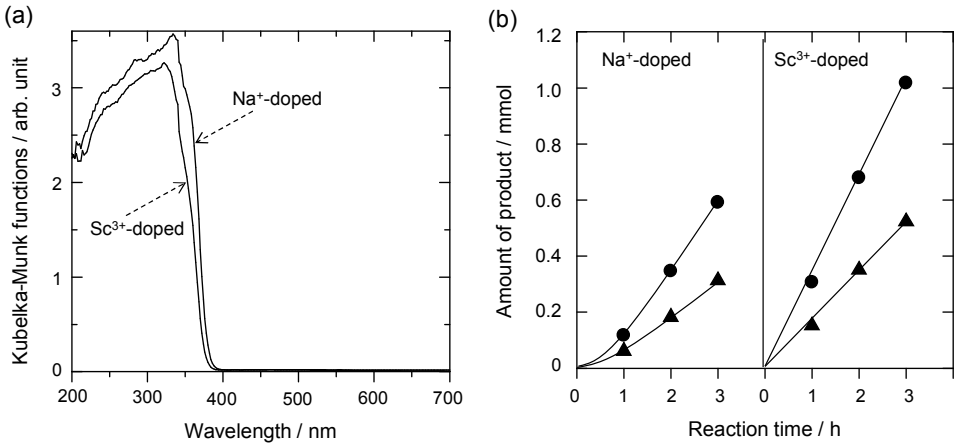

Figure S1 UV-Vis diffuse reflectance spectra (a) and time courses of gas evolution during the water splitting reaction (b) for $SrTiO_3$ samples doped with Na^+ and Sc^{3+}. Catalyst, 0.1 g; solution, cocatalyst, $RhCrO_x$ (0.5+0.5 wt% as Rh_2O_3+Cr_2O_3); H_2O (250 ml); light source, Xe lamp (300 W, full arc). Filled circles, H_2; filled triangles, O_2.

SI2 Long term photoirradiation runs

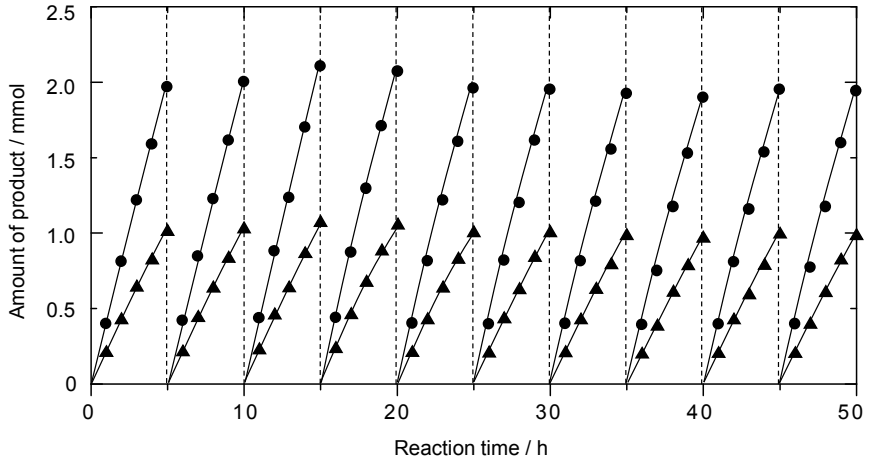

Figure S2 Time course of gas evolution during the long term water splitting reaction on Ta_2O_5(7 wt%)/Rh_2O_3(0.5 wt%)/$SrTiO_3$:Sc. Accumulated gas in the reaction system was removed by evacuation at every 5 h of interval. Catalyst, 0.1 g; solution, H_2O (250 ml); light source, Xe lamp (300 W, full arc). Filled circles, H_2; filled triangles, O_2.

SI3 Photodeposition on Rh/$SrTiO_3$:Sc

First, Rh was photodeposited *in situ* on $SrTiO_3$:Sc as a cocatalyst core by 1 h of photoirradiation from an aqueous solution containing a certain amount of $RhCl_3$ (0.3 wt% as Rh). After that, a certain amount of K_2CrO_4, Ta peroxide solution or Ti peroxide solution (B) was added to the suspension, and Cr_2O_3, Ta_2O_5 or TiO_2 was subsequently photodeposited in a similar manner to the cases of their photodepositions on Rh_2O_3/$SrTiO_3$:Sc.

Although Rh/$SrTiO_3$:Sc showed very poor photocatalytic activity of H_2 and O_2 evolution, overall water splitting proceeded efficiently after the photodeposition in each case as shown in Fig. S3. Among them the TiO_2-photodeposited sample showed the highest photocatalytic activity.

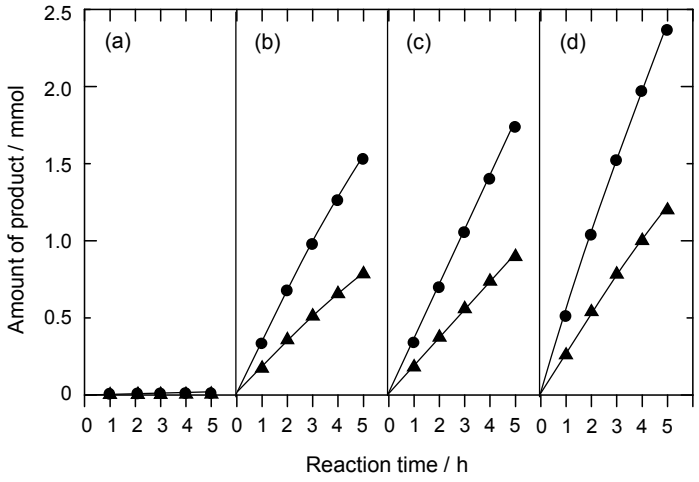

Figure S3 Time courses of gas evolution during the water splitting reaction on photodeposited Rh(0.5 wt%)/$SrTiO_3$:Sc samples. (a) Rh-loading alone, (b) Cr_2O_3(1.0 wt%) photodeposition, (c) Ta_2O_5(5 wt%) photodeposition and (d) TiO_2(5 wt%) photodeposition. Catalyst, 0.1 g; solution, cocatalyst, H_2O (250 ml); light source, Xe lamp (300 W, full arc). Filled circles, H_2; filled triangles, O_2.

SI4 Ex situ photodeposition method

In situ photodeposition of metal oxides from metal peroxide complexes was achieved via photocatalyst excitation. However, the metal oxides may have been deposited via direct photodecomposition of metal peroxides. In order to confirm this effect, another deposition method, referred to as *ex situ* photodeposition, was examined. The details of this method are presented below. Figure S4 shows the time course of O_2 evolution during the photoirradiation of an aqueous Ta peroxide solution in the absence of any photocatalyst. In this case, O_2 evolution occurred and was terminated within 24 h of photoirradiation, at which point the decomposition of all peroxides species was assumed to be completed. After this stage, the photocatalyst powder was added into the aqueous solution, followed by magnetic stirring for a few minutes and evacuation of the gases in the reaction system. Then, the photocatalytic reaction was initiated. This whole sequence is referred to as the *ex situ* photodeposition method. After termination of the photodeposition process, H_2 and O_2 evolved stoichiometrically at a constant rate, exhibiting a photocatalytic activity comparable to that obtained by the *in situ* photodeposition method. This indicates that the direct photodecomposition of peroxides and the subsequent adsorption process, namely *ex situ* photodeposition, are also effective for overall water splitting.

Well-dispersed oxide clusters or nanoparticles, which were nucleated in the aqueous solution by direct photodecomposition of peroxides, were able to adsorb onto the photocatalyst surface to lower the surface energy of the dispersed species.

The O_2 evolution rate during *ex situ* photodeposition was far slower than that during *in situ* photodeposition. Therefore, it can be regarded that the photocatalytic route was likely predominant than the direct photoexcitation route for the decomposition of peroxides in the *in situ* photodeposition process.

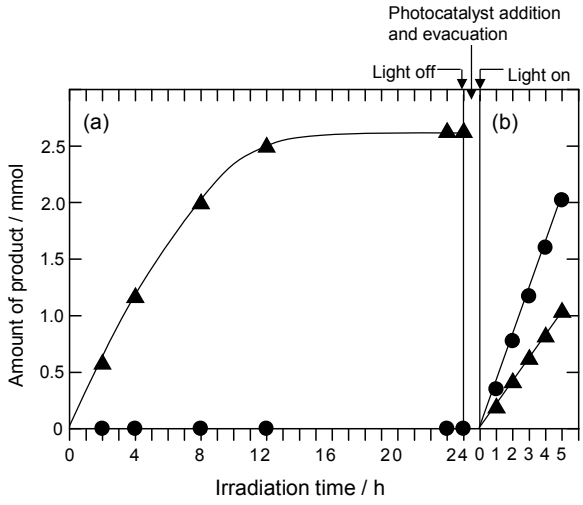

Figure S4 Time courses of gas evolution during the decomposition of Ta peroxide solution (a) and subsequent water splitting reaction (b) on Ta_2O_5(5 wt%)/Rh_2O_3(0.5 wt%)/$SrTiO_3$:Sc. Catalyst, 0.1 g; solution, H_2O (250 ml); light source, Xe lamp (300 W, full arc). Filled circles, H_2; filled triangles, O_2.

SI5 XPS

XPS was measured for the Rh_2O_3(1.0 wt%)/$SrTiO_3$:Sc samples before and after the photodeposition of Ta_2O_5(5 wt%). In Table S1, surface atomic ratios before and after photodeposition are tabulated. After photodeposition, a sufficient amount of the Ta component was detected in the surface composition. On the other hand, the atomic ratios of Ti and Rh decreased substantially upon photodeposition, whereas that of Sr did not decrease as much. In addition, the chemical state of the Sr3d peak clearly changed, as seen in Fig. S5. This indicates that the photocatalyst surface was coated with a Ta_2O_5 layer, but Sr species partly leached into the coating layer. Photoirradiation of the $SrTiO_3$:Sc sample in the presence of H_2O_2 likely resulted in partial elution of the Sr species from the $SrTiO_3$:Sc surface. However, this phenomenon was not responsible for the observed successful water splitting, as demonstrated by the experiment shown in the manuscript (Fig. 2e).

Table S1 Surface atomic ratios of Rh_2O_3(1.0 wt%)/$SrTiO_3$:Sc before and after Ta_2O_5(5 wt%)-photodeposition (PD), determined by X-ray photoelectron spectroscopy.

Sample	Surface atomic ratio (%)				
	O	Sr	Ti	Rh	Ta
Before PD	61.45	18.95	15.21	4.39	0
After PD	67.61	14.99	4.47	1.22	11.71

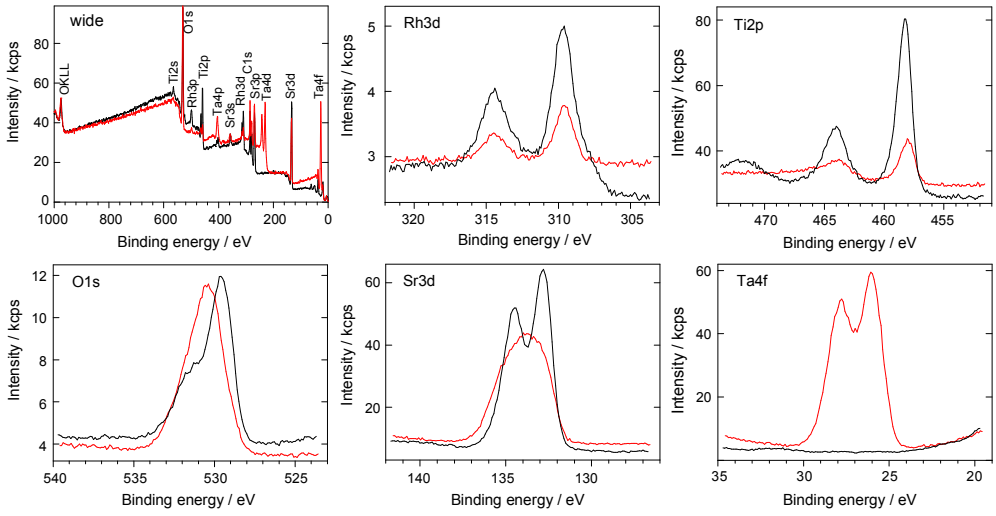

Figure S5 X-ray photoelectron spectra of Rh_2O_3(1.0 wt%)/$SrTiO_3$:Sc before (black line) and after (red line) Ta_2O_5(5 wt%)-photodeposition.

SI6 XRD

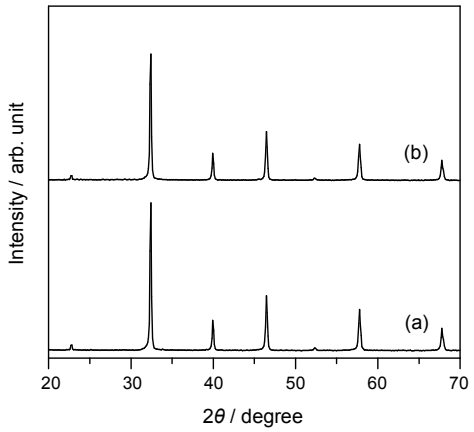

Figure S6 X-ray diffraction patterns of $SrTiO_3$:Sc samples. (a) as-synthesized and (b) Ta_2O_5(15 wt%)/Rh_2O_3(0.5 wt%)-deposited.

SI7 Various coating methods

Some of our results suggested that the photodeposition process may not be indispensable if a fully coated surface structure can be fabricated. Thus, various other coating methods were explored. The results are summarized in Fig. S7. First, a TiO_2 coating obtained by hydrolysis of titanium tetraisopropoxide (TTIP) in EtOH solution with drying on a hot water bath was examined. However, the photocatalytic activity of the 3 wt% TiO_2 coating deposited by this method was found to be far lower than that of the photodeposited sample, although a slight enhancement was observed compared to the case of Rh_2O_3 loading alone. This is probably due to the inhomogeneous coating quality. The photocatalytic activity remained poor upon further TiO_2 deposition (10 wt%) by TTIP hydrolysis, although a slight increase was observed relative to the 3 wt% coating. Then, a TiO_2 coating was fabricated using a different Ti solution, Ti-peroxide solution (A), by a similar manner to the TTIP hydrolysis. In this case, the photocatalytic activity was far higher than in the TTIP case, but roughly half that obtained via photodeposition. The presence of H_2O_2 in the latter Ti solution retarded hydrolysis. The slower hydrolysis of the aqueous Ti peroxide solution yielded a more homogeneous coating, resulting in better photocatalysis.

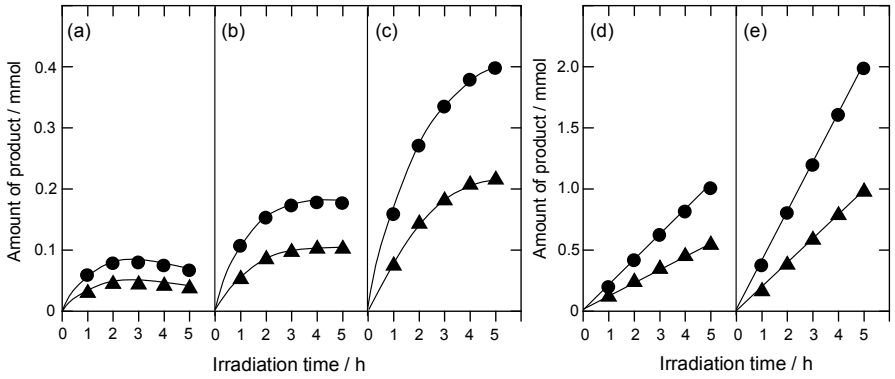

Figure S7 Time courses of H_2 and O_2 evolution during photoirradiation on variously TiO_2-coated Rh_2O_3(0.5 wt%)/$SrTiO_3$:Sc. (a) uncoated, (b) TiO_2(3 wt%)-coated by drying from TTIP/EtOH, (c) TiO_2(10 wt%)-coated by drying from TTIP/EtOH, (d) TiO_2(3 wt%)-coated by drying from aqueous Ti-peroxide solution (A), and (e) TiO_2(3 wt%)-coated by photodeposition from aqueous Ti-peroxide solution (B). Catalyst, 0.1 g; solution, H_2O (250 ml); light source, Xe lamp (300 W, full arc). Filled circles, H_2; filled triangles, O_2.